THE EUROPEAN
PHYSICAL JOURNAL
APPLIED PHYSICS

Regular Article

Does Fourier analysis yield reliable amplitudes of quantum oscillations?

Alain Audouard[1] and Jean-Yves Fortin[2,*]

[1] Laboratoire National des Champs Magnétiques Intenses, UPR 3228 CNRS, INSA, UGA, UPS, 143 avenue de Rangueil, 31400 Toulouse, France

[2] Laboratoire de Physique et Chimie Théoriques, CNRS UMR7019, Université de Lorraine, Vandoeuvre-lès-Nancy 54506, France

Abstract. Quantum oscillation amplitudes of multiband metals, such as high-T_c superconductors in the normal state, heavy fermions or organic conductors, are generally determined through Fourier analysis of the data even though the oscillatory part of the signal is field-dependent. It is demonstrated that the amplitude of a given Fourier component can strongly depend on both the nature of the windowing (either flat, Hahn or Blackman window) and, since oscillations are obtained within a finite field range, the window width. Consequences on the determination of the Fourier amplitudes, hence of the effective masses, are examined in order to determine the conditions for reliable data analysis.

1 Introduction

Quantum oscillations, the extrema of which are periodic in inverse magnetic field, are known to provide valuable information for the study of Fermi surface of metals. In particular, in addition to their frequencies which are directly related to the closed orbit areas on the Fermi surface, field and temperature dependence of their amplitudes allows for the determination of the effective masses and scattering rates [1]. Multiband metals such as heavy fermions [2] or high-T_c superconducting iron chalcogenides [3–6] have a complex Fermi surface due to numerous sheets crossing the Fermi level, giving rise to many orbits under a magnetic field, hence to a complex quantum oscillation spectrum. Besides, in the case where magnetic breakdown (MB) or quantum tunneling of quasi-particles between orbits occurs, as in many organic metals [7,8], additional orbits are further generated. In such cases, data can be readily derived through a Fourier analysis, allowing discrimination between the various frequencies. The point is that the amplitude of quantum oscillations is field dependent. Therefore, strictly speaking, they are not periodic in inverse field. The question that arises is then to determine to what extent reliable temperature- and field-dependent amplitudes can be derived from the Fourier analysis of such field-dependent data.

In the following, we consider the organic metal θ-(ET)$_4$ZnBr$_4$(C$_6$H$_4$Cl$_2$), for which the de Haas–van Alphen (dHvA) and Shubnikov–de Haas (SdH) oscillations were extensively studied [9] in pulsed magnetic fields of up to 55 T. As it is the case of many compounds based on the bis(ethylenedithio)tetrathiafulvalene molecule

(abbreviated as ET), this compound illustrates the model Fermi surface proposed by Pippard to compute magnetic breakdown amplitudes of multiband metals [10]. As reported in reference [9] and depicted in Figure 1, its Fermi surface is composed of one strongly two-dimensional closed orbit (α) and a pair of quasi-one-dimensional sheets giving rise in a magnetic field to the orbit β originated from MB. As a result, the oscillation spectrum is composed of many frequencies which are linear combinations of the frequencies linked to the α and β orbits. Amplitudes relevant to these combinations are strongly influenced by oscillations of the chemical potential in the magnetic field [9,11]. Nevertheless, it appears that this phenomenon has negligible influence on the amplitude of the dominant components α and β, allowing relevant data analysis on the basis of the Lifshitz–Kosevich formalism [12].

Rather than bringing additional information on this compound, the aim of this paper is to determine to what extent the Fourier analysis is able to yield reliable values of physical parameters of interest, in particular effective masses and scattering rates (through the Dingle temperature). To this purpose, we will consider the β orbit [9], with frequency $f_0 = f_\beta = 4534$ T, effective mass $m^* = m_\beta = 3.4\ m_e$ and $T_D = 0.8$ K (this latter parameter being dependent on the considered crystal), and which involves no reflections and four tunnelings with MB field $B_0 = 26$ T. This component will serve as a basis to determine the influence of the windowing (nature and width) on the Fourier amplitude evaluation.

2 Methodology

At a fixed temperature T, a given Fourier component of the oscillatory part of magnetization (dHvA oscillations) and conductivity (SdH oscillations) can be generally written
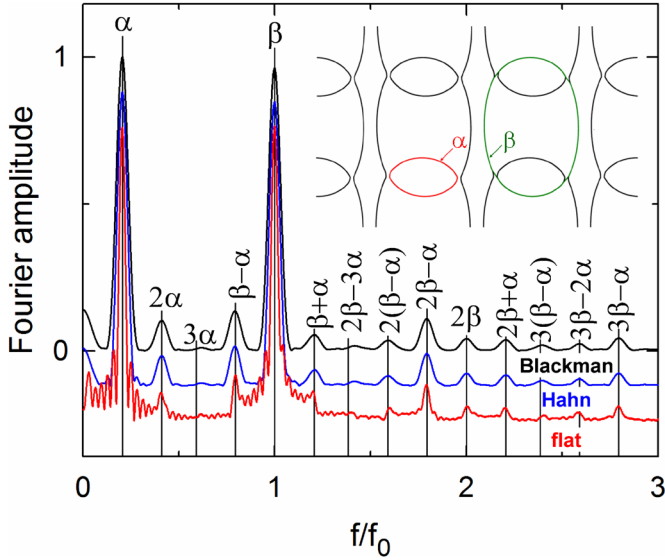
Fig. 1. Fourier analysis of de Haas–van Alphen oscillations of the organic metal θ-$(ET)_4ZnBr_4(C_6H_4Cl_2)$, obtained with Blackman, Hahn and flat windows in the field range 40–56 T at 2 K, see text for details. Vertical lines are marks calculated with $f_\alpha = 930$ T and $f_0 = f_\beta = 4534$ T. The insert displays the Fermi surface in which the α and β orbits are indicated (data are from Ref. [9]).

as $A(x) = A_0(x)\sin(2\pi f_0 x + \phi)$, where $x = 1/B$, f_0 is the frequency and ϕ is, for normal metals, the Onsager phase, generally equal to the product of π and the harmonic number. In the framework of the Lifshitz–Kosevich and Falicov–Stachowiak formalism [1,12,13], the amplitude is given by a product of amplitude damping factors $A_0(x) \propto R_T R_D R_{MB}$ for a given field direction (in which case the spin damping factor is a field- and temperature-independent prefactor). For a two-dimensional orbit, the thermal, Dingle and MB damping factors are given by the expressions $R_T = u_0 T m^* x / \sinh(u_0 T m^* x)$, $R_D = e^{-u_0 T_D m^* x}$ and $R_{MB} = e^{-n_t B_0 x/2}(1 - e^{-B_0 x})^{n_r/2}$, respectively, where $u_0 = 2\pi^2 k_B m_e(e\hbar)^{-1} = 14.694$ T/K, m^* is the effective mass and T_D is the Dingle temperature ($T_D = \hbar/2\pi k_B \tau$, where τ is the relaxation time). n_t and n_r are the number of tunneling and reflections the quasi-particles are facing during their travel along a MB orbit with a MB gap B_0. In the following, we will consider dHvA oscillations relevant to the above-mentioned β orbit. Since measured magnetic torque τ is related to magnetization **M** as $\tau = \mathbf{M} \times \mathbf{B}$, the Fourier amplitude can be written as

$$A_0(x) \propto \frac{T m_\beta}{\sinh(u_0 T m_\beta x)} \exp\left[-(u_0 T_D m_\beta + 2B_0)x\right]. \quad (1)$$

At high-enough values of $u_0 T m^* x$, $A_0(x)$ can be approximated as

$$A_0(x) \simeq a_0 \exp(-\lambda x), \quad (2)$$

where a_0 is a temperature-dependent prefactor ($a_0 \propto T$) and $\lambda = u_0(T + T_D)m_\beta + 2B_0$.[1] This approximation provides a single parameter characterizing the field dependence of the amplitude: the largest the λ, the steepest the field dependence. For θ-$(ET)_4ZnBr_4(C_6H_4Cl_2)$, explored λ values are within 194 T at 2 K and 305 T at 4.2 K. Due to large Dingle temperature, even larger values are obtained for the high-T_c superconductor FeSe, for which λ varies from 250 T at 1.6 K to 370 T at 4.2 K [6].

Since the signal amplitude is field-dependent, windowing [14–18] is mandatory in order to determine the Fourier amplitude at a given inverse field value $\overline{x}$. The inverse field range Δx is within x_m and x_M ($\Delta x = x_M - x_m$) and centered on $\overline{x} = (x_m + x_M)/2$. In order to explore the influence of windowing on the Fourier amplitude, flat, Hahn and Blackman windows are considered in the following: $w(x) = 1$, $w(x) = \{1 + \cos[2\pi(x - \overline{x})/\Delta x]\}/2$, and $w(x) = 0.42 + 0.5\cos[2\pi(x - \overline{x})/\Delta x] + 0.08\cos[4\pi(x - \overline{x})/\Delta x]$, respectively, within the range x_m to x_M and $w(x) = 0$ everywhere else. We can write more generally the window function as $w(x) = \sum_{n \geq 0}^{p} c_n \cos[2\pi n(x - \overline{x})/\Delta x]$, where $p = 0$, 1, 2 for a flat, Hahn and Blackman window, respectively, but this can be generalized for higher values of p with appropriate coefficients. Discrete Fourier transforms are obtained as

$$F(f,\overline{x}) = \frac{2}{\Delta x} \int_{x_m}^{x_M} A_0(x) \sin(2\pi f_0 x + \phi)w(x)$$
$$\exp(-2i\pi f x)\mathrm{d}x. \quad (3)$$

Analytical solution of equation (3) is given in the Appendix (Eq. (A.5)) for $f = f_0$. The modulus of $F(f_0, \overline{x})$ defines the Fourier amplitude $A_F(\overline{x}) = |F(f_0, \overline{x})|/c_0$. For finite λ and $f_0 \gg \lambda$, equation (A.4) holds, yielding

$$A_F(\overline{x}) = A_0(\overline{x})c_0^{-1} \frac{\sinh(\lambda \Delta x/2)}{\lambda \Delta x/2}$$
$$\times \sum_{n=0}^{p}(-1)^n c_n \frac{(\lambda \Delta x/2)^2}{(\lambda \Delta x/2)^2 + \pi^2 n^2}. \quad (4)$$

$A_F(\overline{x})$ can also be obtained by numerical resolution of equation (3), where $A_0(\overline{x})$ is either given by equation (2) or by experimental data of reference [9]. Available frequencies are bounded by the Raleigh frequency ($f_{\min} = 1/\Delta x$) and by the Nyquist frequency ($f_{\max} = 1/2\delta x$, for data sampled at evenly spaced δx values). Accordingly, Δx is kept above $1/f_0$, and δx is always small enough to ensure that $f_{\max}$ is much higher than f_0 [19].

3 Results and discussion

The Fourier analysis displayed in Figure 1 shows that the largest (smallest) secondary lobes and the smallest (largest) peak width are obtained for the flat (Blackman)

---

[1] At the lowest temperature (2 K) and highest field (55 T), i.e. lowest $u_0 T_m \beta_x$ values explored in reference [9], this approximation overestimates the amplitude of the considered β component by less than 3%. Accordingly, the relevant reported mass plots are linear (see also Fig. 4a).
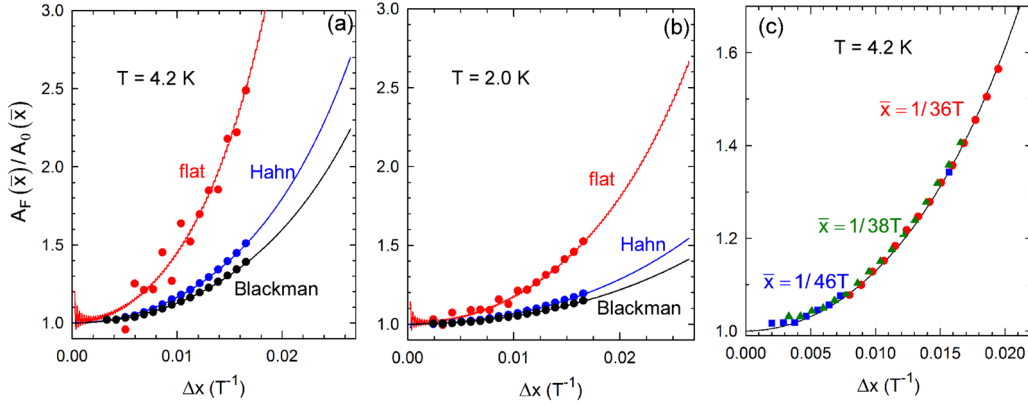
Fig. 2. Fourier amplitude $A_F(\overline{x})$ relevant to the β component of the organic metal θ-$(ET)_4ZnBr_4(C_6H_4Cl_2)$ at (a) 4.2 K ($\lambda = 305$ T) and (b) 2.0 K ($\lambda = 194$ T), normalized to the oscillation amplitude predicted by the Lifshitz–Kosevich formula $A_0(\overline{x})$ as a function of the inverse field window Δx for flat, Hahn and Blackman windows, at $\overline{x} = 1/38$ T and (c) for Blackman window at various $\overline{x}$ values. Solid symbols are deduced from experimental data reported in Ref. [9]. Solid lines are obtained from numerical resolutions of equation (3).

window, while the Hahn window provides intermediate behaviour, as widely reported [14–18].

Discrepancy between amplitude $A_F(\overline{x})$ deduced from the Fourier analysis within a finite field range $1/x_M$ to $1/x_m$ and the actual Fourier amplitude $A_0(\overline{x})$ given by equation (2) can be evaluated through the ratio $A_F(\overline{x})/A_0(\overline{x})$, which should be equal to 1. According to the data in Figure 2, a strong increase of this ratio is observed as Δx increases. Furthermore, for a given window width Δx, it increases as λ increases, e.g. by increasing the temperature, while as the mean magnetic field $(1/\overline{x})$ decreases, it grows staying on the same curve, as reported in Figure 2c. The most dramatic effect is observed for the flat window, indicating that smooth windowing is necessary to get amplitudes as reliable as possible since, more specifically, $A_F(\overline{x})/A_0(\overline{x})$ grows as $A_F(\overline{x})/A_0(\overline{x}) \simeq \sinh(\lambda\Delta x/2)/(\lambda\Delta x/2)$ in this case.

In line with equation (4), the ratio $A(\overline{x})/A_0(\overline{x})$ depends only on the product $\lambda\Delta x$ for a given window type. Hence, strictly speaking, the Fourier analysis yields reliable amplitudes for finite Δx in the case of field-independent signal ($\lambda = 0$) only. Unfavourably, moderate oscillations of the Fourier amplitude is however observed for small Δx, in particular for the flat window. It can be checked that these oscillations are periodic in Δx, their frequency being just f_0, in agreement with equation (A.5). This feature brings us to consider the influence of the quantum oscillation frequency on the data. As reported in Figure 3, the Fourier amplitude $A_F(\overline{x})$ is dominated by the monotonous term of equation (A.5), yielding equations (A.4) and (4), in the case of large-enough frequency and Δx. In contrast, large oscillations of both the Fourier amplitude and the frequency of the Fourier peaks (which is no more equal to f_0 in this case) are observed for low frequencies.

This effect is relevant in the case of slow magnetic oscillations, such as superconducting iron-based chalcogenides [3–6] and in semimetal $BaNiS_2$ [20], where frequencies as low as 37 T are reported. Also, slow frequency phenomena are present in magnetoresistance

oscillations of organic conductors [21] or high-T_c superconductors [22] due to the mixing of two close frequencies, the amplitude of which is still in debate [21]. In these cases, Fourier amplitudes can depend strongly on the windowing process.

In addition, whereas only the envelope of $A_F(\overline{x})$, i.e. $A_0(\overline{x})$, is relevant for the Fourier amplitude at high Δx, Onsager phase-dependent data are observed in Figure 3 for low frequencies. In short, Δx must be both small enough to avoid the amplitude overestimation predicted by equation (A.5) and large enough to avoid the undulations reported in Figure 3 in this case. As a consequence, reliable data can hardly been deduced from the Fourier analysis of low-frequency quantum oscillations.

Since λ depends on temperature, the discrepancy between the actual and Fourier amplitudes for large Δx depends on temperature as well. This may lead to a significant error on the effective mass deduced from temperature dependence of the amplitude (the so-called mass plot), as evidenced in Figure 4a, and hence on the determination of the scattering rate through Dingle plots as well. As reported in Figure 4b and c, underestimation of m_β by about 30% is obtained for a flat window at $\overline{x} = 1/32$ T^{-1} for $\Delta x = 0.026$ T^{-1} (i.e. in the field range 23–56 T). About 50% would be reached at $\overline{x} = 1/56$ T^{-1} for the same Δx value (field range within 32 and 193 T). Smaller although significant errors are obtained for Hahn (not shown) and Blackman windows, e.g. 15 and 13%, respectively, for $\overline{x} = 1/32$ T^{-1} and $\Delta x = 0.026$ T^{-1}.

4 Conclusion

Amplitude of field-dependent quantum oscillations deduced from the Fourier analysis is overestimated even though it is widely used, as reported in the literature. Analytical formulas accounting for this phenomenon are discussed in this manuscript. Most dramatic effects are observed for steep field-dependent amplitudes
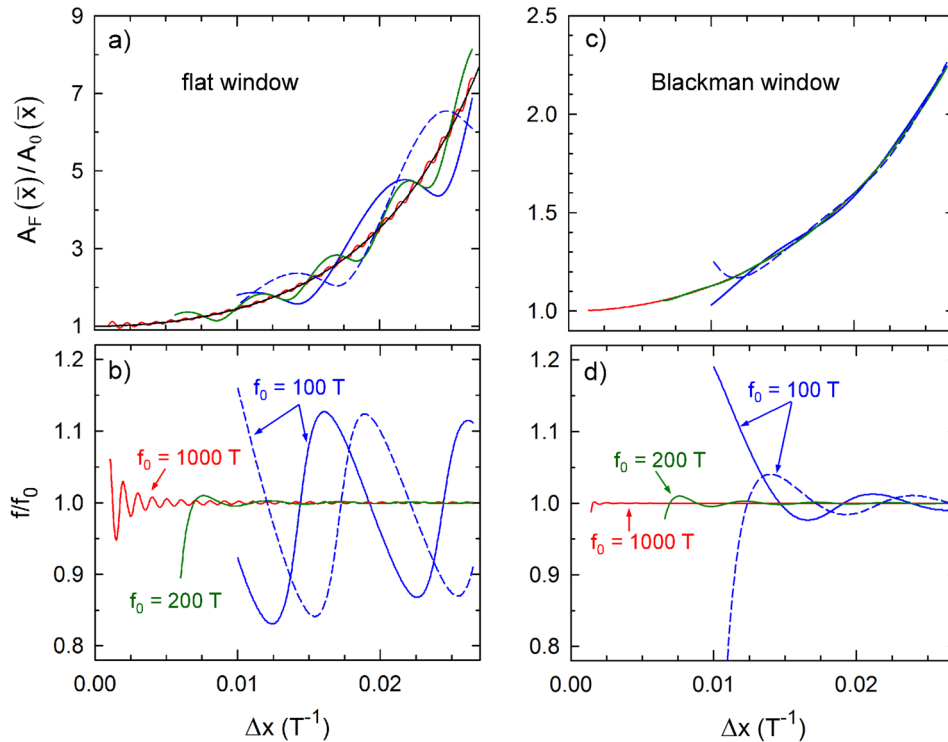
Fig. 3. Inverse field window width (Δx) dependence of (a), (c) Fourier amplitude and (b), (d) frequency for (a), (b) flat and (c), (d) Blackman window for various oscillation frequencies f_0 and $\lambda = 305$ T. The Onsager phase is $\phi = 0$ and $\phi = \pi$ for solid and dashed lines, respectively. Black solid line in (a) stands for equation (4).
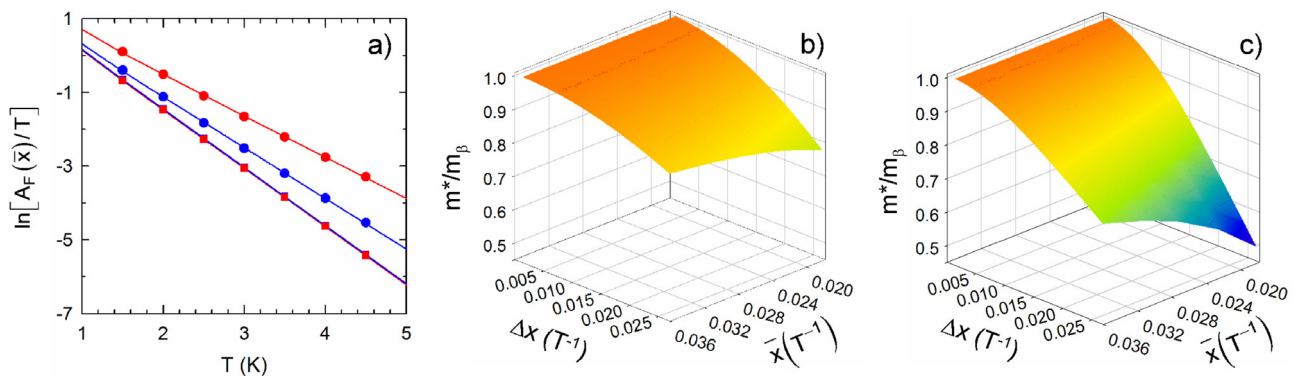
Fig. 4. (a) Mass plots relevant to the β component of the organic metal θ-$(ET)_4ZnBr_4(C_6H_4Cl_2)$, with effective mass $m_\beta = 3.44$, deduced from the Fourier analysis for $\overline{x} = 1/32$ T, in the temperature range 1.5–4.5 K. Blue and red symbols are data obtained with Blackman and flat windows, respectively. Solid squares and circles are data for $\Delta x = 0.00093$ T^{-1} and 0.0265 T^{-1}, respectively. Solid lines are best fits to the Lifshitz–Kosevich formula. For large Δx, both the Fourier amplitude increases and the slope decreases yielding underestimated effective mass. Such fittings yield data of Figure 4b and c, where the effective mass is plotted versus the inverse field window width (Δx) and mean inverse field value ($\overline{x}$) for (b) Blackman and (c) flat window. At high field (i.e. small $\overline{x}$) and large field window width (Δx), strong underestimation of the effective mass is obtained.

determined using flat windows with large width. Nevertheless, acceptable discrepancy with actual amplitude is obtained with Blackman window of moderate width for high-enough frequencies. In contrast, oscillations with low frequencies such as that observed in iron-based chalcogenides superconductors must be considered with care since Δx must be both small enough to avoid overestimated amplitude and large enough to avoid spurious effects observed coming close to the inverse of the Raleigh frequency.

Author contribution statement

A. Audouard developed the idea of analysing the amplitudes of the quantum oscillations extracted from Fourier algorithms, in order to estimate their influence on the physical parameters. J.-Y. Fortin helped in writing the different formulas used in this analysis.

Appendix: Analytical expression of the Fourier transforms

In general, we can write the window function $w(x) = \sum_{n \geq 0}^{p} c_n \cos[2\pi n(x - \overline{x})/\Delta x]$, where $p = 0$, 1, 2 stands for a flat, Hahn and Blackman window, respectively, and the condition $\sum_{n=0}^{p} c_n = 1$. These coefficients are given numerically by $\{c_0 = 1\}_{\text{Flat}}$, $\{c_0 = 0.5, c_1 = 0.5\}_{\text{Hahn}}$ and $\{c_0 = 0.42, c_1 = 0.5, c_2 = 0.08\}_{\text{Blackman}}$. Equations (2) and (3) lead to

$$F(f_0, \overline{x}) = \frac{1}{\Delta x} \sum_{n=0}^{p} c_n \sum_{\varepsilon = \pm 1}$$
$$\times \int_{x_m}^{x_M} A_0(x) \sin(2\pi f_0 x + \phi) e^{-2i\pi f_0 x - 2i\pi n\varepsilon(x - \overline{x})/\Delta x} dx \tag{A.1}$$

for $f = f_0$, $x = \overline{x} = (x_M + x_m)/2$ and $A_0(x) = a_0 e^{-\lambda x}$. Writing $F(f_0, \overline{x}) = \sum_n c_n \sum_{\varepsilon = \pm 1} F_{n\varepsilon}$ in equation (A.1), one can compute individually $F_{n\varepsilon}$, which leads after integration to

$$F_{n\varepsilon} = \frac{2a_0 e^{2i\pi n\varepsilon \overline{x}/\Delta x + i\phi}}{i\Delta x}$$
$$\times \left[e^{-\lambda_{n\varepsilon} \overline{x}} \frac{\sinh(\lambda_{n\varepsilon} \Delta x/2)}{\lambda_{n\varepsilon}} - e^{-\Lambda_{n\varepsilon} \overline{x}} \frac{\sinh(\Lambda_{n\varepsilon} \Delta x/2)}{\Lambda_{n\varepsilon}} \right], \tag{A.2}$$

where we have defined $\lambda_{n\varepsilon} = \lambda + 2i\pi n\varepsilon/\Delta x$ and $\Lambda_{n\varepsilon} = \lambda + 4i\pi f_0 + 2i\pi n\varepsilon/\Delta x$. This expression does not depend on ϕ up to a global sign, for the values $\phi = 0$, π. Assuming $f_0 \gg \lambda$, only the first term in bracket will contribute to $F_{n\varepsilon}$. Since $\sinh(\lambda_{n\varepsilon}\Delta x/2) = (-1)^n \sinh(\lambda \Delta x/2)$, one obtains

$$F_{n\varepsilon} \simeq \frac{2a_0 e^{-\lambda \overline{x} + i\phi}}{i\Delta x}(-1)^n \frac{\sinh(\lambda \Delta x/2)}{\lambda + 2i\pi n\varepsilon/\Delta x}. \tag{A.3}$$

After summing over ε, the Fourier transform is finally equal to

$$F(f_0, \overline{x}) \simeq$$
$$- iA_0(\overline{x}) e^{i\phi} \frac{\sinh(\lambda \Delta x/2)}{\lambda \Delta x/2} \sum_{n=0}^{p} (-1)^n c_n \frac{(\lambda \Delta x/2)^2}{(\lambda \Delta x/2)^2 + \pi^2 n^2}. \tag{A.4}$$

The exact formula is obtained by incorporating the contribution from the second term of equation (A.2), involving $\Lambda_{n\varepsilon}$ and which induces oscillations as a function of

$\overline{x}$ and Δx, with frequency f_0

$$F(f_0, \overline{x}) = - iA_0(\overline{x}) e^{i\phi} \sum_{n \geq 0} (-1)^n c_n$$

$$\left[\frac{\sinh(\lambda \Delta x/2)}{\lambda \Delta x/2} \frac{(\lambda \Delta x/2)^2}{(\lambda \Delta x/2)^2 + \pi^2 n^2} - e^{-4i\pi f_0 \overline{x}} \right.$$

$$[\cos(2\pi f_0 \Delta x) \sinh(\lambda \Delta x/2)$$
$$+ i \sin(2\pi f_0 \Delta x) \cosh(\lambda \Delta x/2)]$$
$$\left. \frac{(\lambda + 4i\pi f_0)\Delta x/2}{\{(\lambda + 4i\pi f_0)\Delta x/2\}^2 + \pi^2 n^2} \right]. \tag{A.5}$$

As Δx goes to zero for finite λ in equation (A.4), it yields the Fourier amplitude $|F(f_0, \overline{x})| \simeq A_0(\overline{x})c_0$. As a result, one defines $A_F(\overline{x}) = |F(f_0, \overline{x})|/c_0$ in order to normalize the function with respect to $A_0(\overline{x})$ in this limit. While $\sinh(\lambda \Delta x/2)/(\lambda \Delta x/2)$ goes to 1 as Δx goes to zero, the other contributions in equation (A.5), which involve oscillatory terms periodic in Δx with the frequency f_0, grow simultaneously. They are responsible for the oscillatory behaviour reported in Figures 2 and 3. In particular, in this limit, if we take into account all the contributions in equation (A.5), one obtains

$$\lim_{\Delta x \to 0} F(f_0, \overline{x}) \simeq 2c_0 A_0(\overline{x}) e^{i\phi - 2i\pi f_0 \overline{x}} \sin(2\pi f_0 \overline{x}). \tag{A.6}$$

Furthermore, as discussed in Section 2, $A_F(\overline{x})/A_0(\overline{x})$ depends only on λ at a given Δx.

References

1. D. Shoenberg, *Magnetic Oscillations in Metals* (Cambridge University Press, Cambridge, UK, 1984)
2. Y. Onuki, R. Settai, Low Temp. Phys. **38**, 89 (2012)
3. T. Terashima, N. Kikugawa, A. Kiswandhi, E.-S. Choi, J.S. Brooks, S. Kasahara, T. Watashige, H. Ikeda, T. Shibauchi, Y. Matsuda, T. Wolf, A.E.B. Böhmer, F. Hardy, C. Meingast, H.V. Löhneysen, M.-T. Suzuki, R. Arita, S. Uji, Phys. Rev. B **90**, 144517 (2014)
4. M.D. Watson, T.K. Kim, A.A. Haghighirad, N.R. Davies, A. McCollam, A. Narayanan, S.F. Blake, Y.L. Chen, S. Ghannadzadeh, A.J. Schofield, M. Hoesch, C. Meingast, T. Wolf, A.I. Coldea, Phys. Rev. B **91**, 155106 (2015)
5. M.D. Watson, T. Yamashita, S. Kasahara, W. Knafo, M. Nardone, J. Béard, F. Hardy, A. McCollam, A. Narayanan, S.F. Blake, T. Wolf, A.A. Haghighirad, C. Meingast, A.J. Schofield, H.V. Löhneysen, Y. Matsuda, A.I. Coldea, T. Shibauchi, Phys. Rev. Lett. **115**, 027006 (2015)
6. A. Audouard, F. Duc, L. Drigo, P. Toulemonde, S. Karlsson, P. Strobel, A. Sulpice, EPL **109**, 27003 (2015)
7. S. Uji, J.S. Brooks, *Springer Series Material Science* (Springer, New York City, 2008), Vol. 110, p. 89
8. A. Audouard, J.-Y. Fortin, C. R. Phys. **14**, 15 (2013)
9. A. Audouard, J.-Y. Fortin, D. Vignolles, R.B. Lyubovskii, L. Drigo, G.V. Shilov, F. Duc, E.I. Zhilyaeva, R.N. Lyubovskaya, E. Canadell, J. Phys. Condens. Matter **27**, 315601 (2015)
10. A.B. Pippard, Proc. R. Soc. Lond. **A270**, 1 (1962)

11. A. Audouard, J.-Y. Fortin, D. Vignolles, R.B. Lyubovskii, L. Drigo, F. Duc, G.V. Shilov, G. Ballon, E.I. Zhilyaeva, R.N. Lyubovskaya, E. Canadell, EPL **97**, 57003 (2012)
12. I.M. Lifschitz, A.M. Kosevich, Sov. Phys. JETP **2**, 636 (1956)
13. L.M. Falicov, H. Stachowiak, Phys. Rev. **147**, 505 (1966)
14. A.S. Filler, J. Opt. Soc. Am. **54**, 762 (1964)
15. J. Allen, IEEE Trans. Acoust. Speech Signal Process. ASSP-**25**, 235 (1977)
16. F.J. Harris, Proc. IEEE **66**, 51 (1978)
17. F.S. Acton, *Numerical Methods That Work* (The Mathematical Association of America, Washington D.C., 1990)
18. D.A. Naylor, M.K. Tahic, J. Opt. Soc. Am. A **24**, 3644 (2007)
19. L. Drigo, F. Durantel, A. Audouard, G. Ballon, Eur. Phys. J. Appl. Phys. **52**, 10401 (2010)
20. Y. Klein, M. Casula, D. Santos-Cottin, A. Audouard, D. Vignolles, G. Fve, V. Freulon, B. Plaçais, M. Verseils, H. Yang, L. Paulatto, A. Gauzzi, Phys. Rev. B **97**, 075140 (2018)
21. P.D. Grigoriev, T.I. Mogilyuk, Phys. Rev. B **95**, 195130 (2017)
22. P.D. Grigoriev, T. Ziman, Phys. Rev. B **96**, 165110 (1017)